Accepted Manuscript

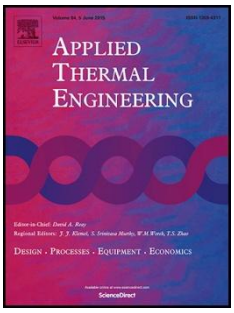

Title: Solid oxide fuel cell performance comparison fuelled by methane, MeOH, EtOH and gasoline surrogate C_8H_{18}

Author: Vincenzo Liso, Giovanni Cinti, Mads Pagh Nielsen, Umberto Desideri

PII: S1359-4311(15)01425-8
DOI: http://dx.doi.org/doi: 10.1016/j.applthermaleng.2015.12.044
Reference: ATE 7458

To appear in: *Applied Thermal Engineering*

Received date: 9-4-2015
Accepted date: 15-12-2015

Please cite this article as: Vincenzo Liso, Giovanni Cinti, Mads Pagh Nielsen, Umberto Desideri, Solid oxide fuel cell performance comparison fuelled by methane, MeOH, EtOH and gasoline surrogate C_8H_{18}, *Applied Thermal Engineering* (2016), http://dx.doi.org/doi: 10.1016/j.applthermaleng.2015.12.044.

Solid oxide fuel cell performance comparison fuelled by methane, MeOH, EtOH and gasoline surrogate C_8H_{18}

Vincenzo Liso[1a]; Giovanni Cinti[b]; Mads Pagh Nielsen[a]; Umberto Desideri[b]

[a]Department of Energy Technology, Aalborg University, Aalborg 9220, Denmark;

[b]Department of Industrial Engineering, University of Perugia, Italy;

Abstract:

Carbon deposition is a major cause of degradation in solid oxide fuel cell systems. The ability to predict carbon formation in reforming processes is thus absolutely necessary for stable operation of solid oxide fuel cell systems.
In the open literature it is found that thesteam input is always considered in large excess compared to what required by the reforming process with the purpose of reducing carbon formation and avoiding rapid degradation of the cell performance. This makes it difficult to consistently compare system performance with different fuels. In this work, the molar compositions at equilibrium is calculated for a minimum steam to carbon ratio for each fuel type.
We carry out a thermodynamic analysis of fuel/steam system, using Gibbs Free Energy minimization method. A mathematical relationship between Lagrange's multipliers and carbon activity in the gas phase was deduced. Minimum steam required for the reforming process for each fuel was related to the heat required for the reforming process and fuel cell open circuit voltage.
Furthermore, in an experimental test, steam reforming product compositions were used to evaluate and compare SOFC performance with different hydrocarbons.
Comparing the model to the experimental activity, it is revealed that at temperatures exceeding 800°C the gas composition is dominated by hydrogen and carbon monoxide for any of the fuels considered leading to similar cell polarization curves performance for different fuels.
The main effect on the performance is related to OCV values which are dependent on different steam content for each fuel. It was concluded that the magnitude of the heat requested for the fuel reforming process is the major difference in system performance when comparing different fuels. However, reforming kinetic effects can become predominant rather than thermodynamics, especially at lower temperatures.

Keywords: Fuel steam reforming; Carbon formation; SOFC systems

Nomenclature

a	species activity
G	gibbs free energy, J/mol
E	Moles of each chemical elements
F	Faradays constant, Coulomb/mol
h , H	Entalphy, J/mol

[1]Author to whom correspondence should be addressed; E-Mail vli@et.aau.dk

n number of moles
n_e number of electrons transferred in the electrochemical reaction
R ideal gas constant, J/(mol K)
S/C steam-to-carbon ratio
T temperature, K
y molar fraction
s entropy
$SOFC$ solid oxide fuel cell

Greek letters

μ chemical potential, J/mol
η fuel cell theoretical efficiency
φ Lagrange function
λ Lagrange undetermined multiplier

Subscript

i molecule or gas species
j chemical element

1. Introduction

A solid oxide fuel cell stack (SOFC) is a promising technology for the conversion of chemical energy into electricity and heat. Due to the high temperature operation, this type of fuel cell can use different fuels such as natural gas, alcohols and gasoline. In particular, alcohols such as methanol or ethanol can be produced by renewable energy sources. In comparison with hydrogen, alcohols have the advantage of easy storage and safe handling. Alcohols show a reasonable energy density and may be appropriate particularly for applications in remote areas not covered by the electrical grid. Natural gas and gasoline have the advantage of the existing distribution and dispensing infrastructure.

In order to operate the cell, the fuel must be converted into hydrogen and lower the content of higher hydrocarbons in a pre-reformer or in the anode channel. Despite for SOFC-based system, complete internal reforming has been demonstrated to be possible, most systems for stationary application favor external pre-reforming, because it yields the highest amount of hydrogen [1],[2]and [3].

For the pre-reforming process, steam reforming is considered one of best options since it delivers the highest hydrogen yield. However, carbon deposition can cause catalyst deactivation both in the reformer and fuel cell [4]. For this reason, thermodynamic analyses have been carried out in many studies to predict conditions under which carbon formation is inhibited during steam reforming [5][6].

It is demonstrated that carbon deposition can be minimized by providing sufficient H_2O in the fuel stream. However, steam generation increases system complexity and control. Therefore it is important from operational

standpoint to identify operating conditions that avoid carbon formation and maximizes the hydrogen yield while simultaneously minimizing the heat input required for steam generation and the endothermic reforming process [4,5].

Previous studies have focused on carbon deposition in reforming processes and at SOFC level. In particular, in [9,10] the cell performance for different fuels, namely methane, methanol, ethanol and gasoline was analyzed by using chemical equilibrium models. Besides, an extensive theoretical and experimental work on fuel options for SOFC was carried out by Sasaki et al. in four reports [6–9]. System considerations were not included in these works. On the other hand when systems based on SOFC are analyzed, only nominal operating conditions for temperature and steam to carbon ratio in the pre-reformer and fuel cell are considered [15],. In this case the most representative values based on those available in open literature are chosen.

In this work the reformation of different fuels for SOFC systems are compared using chemical equilibrium and system level analysis are drawn. The thermodynamic conditions for carbon formation are examined through the analysis of carbon activity in the reformate gas. A mathematical relationship between Lagrange's multipliers and the carbon activity, with reference to the graphite phase, is deduced, enabling to calculate the carbon activity in the reformer gas. From this, it is possible to predict if carbon will precipitate inside the reformer.

In most cases the equilibrium in steam reforming process is analyzed for a fixed and optimal steam to carbon ratio at different temperature (e. g. research work in [12,13, 16]). Depending on the fuel, steam input is always in excess with the purpose of reducing the risk of carbon formation. This makes difficult to consistently compare the reforming of different fuels in a system. In this work the molar compositions at equilibrium are calculated for a minimum steam to carbon ratio, making it easier to compare different fuels. For each fuel composition, the heat input for the endothermic reforming process is estimated and the fuel cell performance is calculated in terms of electromotive force EMF and maximum cell efficiency.

2. Methodology

Different mathematical methods were developed to explain and predict the behavior of solutions in dynamic equilibrium. Minimization of the Gibbs free energy and the law of mass action are among the most used especially in numerical simulations [17].

The Gibbs free energy minimization approach was introduced in 1958 by White, Johnson and Dantzig in [18]; since then it has been used in most computer programs for chemical equilibrium calculations for its ability to generalize any reaction scheme (e.g. combustion, reforming). The law of mass action, on the other hand, requires

that the stoichiometric reaction scheme is known. The two methods produce similar results.

In this study, the Gibbs free energy minimization was applied to analyze thermodynamic equilibrium of steam reforming of different fuels. The equilibrium conversion of CH_4, MeOH, EtOH and C_8H_{18} was studied in the temperature of range of 250°C to 1000°C. It should be noted that complete thermodynamic equilibrium was assumed. However, a deviation of the chemical composition may be registered in a reforming reactor due to slow kinetics of the steam reforming reactions.

For simplicity, only following species were considered in the calculations in this study:H_2(g), H_2O(g), O_2(g), CO(g), CO_2(g), CH_4(g), solid graphite C, n-C_8H_{18} and alcohols CH_3OH and C_2H_5OH. Methane was chosen as representative of natural gas as it is its main constituent while n-octane and its isomers were considered to represent thermodynamic properties of gasoline. The model was developed in EES and the results were validated using CEA-NASA, a program which calculates chemical equilibrium product concentrations from any set of reactants and determines thermodynamic properties for the product mixture based JANAF thermochemical database. The total pressure considered for this simulation was 1 bar. Partial pressures were derived from the chemical compositions by assuming fuel gas species as ideal. As steam generation requires a significant energy input, the heat required to elevate the temperature of reactants (i.e. fuel and steam) to the reforming temperature was estimated.

Compared to the CEA-Nasa software package, the mathematical formulation based on the Lagrange Method of Undetermined Multipliers can be reproduced in any numerical equation solver making this option more adaptable to different software platforms. The mathematical formulation has also the advantage to explicitly impose zero thermodynamic carbon activity (i.e. no carbon formation).

In order to consistently compare the amount of steam required in the reforming process for different fuels, the minimum steam-to-carbon ratio which inhibits carbon formation was calculated using at each temperature. This is obtained imposing zero thermodynamic carbon activity in the steam reforming equilibrium model.

Even though the reforming process is usually achieved for different fuels at different temperatures, we have assumed one temperature of reforming for all types of fuel. In fact as the reforming process is comprised of mainly equilibrium limited reactions, the high temperature in the cell channels, would lead to complete the reforming process reactions.

The electromotive force represents the open circuit voltage. The irreversible voltage loss (i.e. activation, ohmic and concentration polarizations) is mainly a function of current density and stack temperature. Since these

parameters are equivalent in each stack and the main scope of this research is a thermodynamic comparison of different fuels, it was assumed that the EMF is a good indicator of the fuel cell performance.

3. Thermodynamic model definition and validation

Model definition

The equilibrium state of a chemical reactive system is characterized by a minimum value of the total Gibbs free energy of a reactants and products mixture at a specified temperature and pressure. If it is assumed that the condensed species possess negligible volume compared to the gas phase in a chemical product mixture, the equation of state for the product species can be simplified by assuming ideal gas behaviour for the entire mixture (i.e. $PV = nRT$).

If the mixture obeys the ideal gas law, the Gibbs free energy of a mixture can be expressed by the product of the chemical potential, μ_i , and the number of mole, n_i , of each $i-th$ gas species.

$$G = \sum_{i=1}^{C} n_i \mu_i \tag{1}$$

The chemical potential of an ideal gas mixture is defined as:

$$\mu_i = \mu_i^o + R_{Univ} T \ln\left(\frac{y_i P}{P^o}\right) \tag{2}$$

where μ_i^o is the chemical potential of $i-th$ species at temperature T and standard state pressure P° , which is normally chosen to be 1 atm, and can be expressed as:

$$\mu_i^o = h_i^o - T s_i^o \tag{3}$$

$y_i P / P^o$ in Eq (2) represents the activity, a_j for each of the species, namely C, H and O:

$$a_i = \frac{y_i P}{P^o} \tag{3}$$

a_i can be used to study the carbon deposition. In particular if carbon activity, a_c , is greater than unity, the gas phase in not in equilibrium and carbon deposition may occur. If carbon activity is less than one, carbon

formation will be not feasible [19].

As solid carbon, only graphite was taken into account for simplicity, whereas various carbon-based materials such as amorphous carbon, carbon nanotubes, and carbon nanofibers could have slightly different thermochemical properties [20].

When solid carbon (Graphite) is involved in the system, the chemical equilibrium takes place between substances in more than one phase. As the solid species does not contribute to the system pressure, the Gibbs free energy can be assumed equal to the standard Gibbs free energy of formation, i.e. $\mu_{C(S)} = \mu^{o}_{C(S)}$.

Therefore the member of moles of each atom that is present (E_j) can be determined. The number of moles must to remain constant as required by mass conservation law. The initial number of moles of each element is given by:

$$E_{0,j} = \sum_{i=1}^{C} n_{0,i} e_{i,j} \qquad \text{for j=1…E} \tag{4}$$

where $n_{0,i}$ is the initial number of moles of each substance and $e_{i,j}$ is the number of moles of the element j in a mole of substance I , and E is the total number of atoms. The number of mole at equilibrium is:

$$n = \sum_{i=1}^{C} n_i \tag{5}$$

and the molar fraction of each gas component is given by:

$$y_i = \frac{n_i}{n} \qquad \text{i=1…C} \tag{6}$$

The Lagrange Method of Undetermined Multipliers is implemented by the following to equations:

$$\varphi_j = \sum_{j=1}^{C} n_i e_{i,j} - E_{0,j} = 0 \quad \text{for j=1…E} \tag{6}$$

$$\mu_i + \sum_{j=1}^{E} \lambda_j e_{i,j} = 0 \quad \text{for i=1…C} \tag{6}$$

The nonlinear system (Eqs. 1-8) was solved by using the Newton-Raphson method implement in EES,

Engineering Equation Solver. As this problem is convex, the global minimum of this equation system is independent from the initial guess values [21].

Remembering that $\mu_i = G_i^0 + RT \ln a_i$, we can calculate the carbon activity in the reforming process using Eq. (6) as follows:

$$a_c = e^{-\left(\mu_C^0 + \lambda_C\right)/RT} \tag{6}$$

The overall reforming mechanism can be divided in three reactions: the endothermic steam reforming reaction (8), and the exothermic methanation reaction and the slightly exothermic water gas shift reaction (9):

$$C_a H_b O_c + s/c\, H_2O \rightleftarrows n_{CO} CO + n_{H_2} H_2 + n_{H_2O} H_2O + n_{CH_4} CH_4 \qquad \Delta H_{298K} > 0 \tag{7}$$

Methanation reaction:

$$CO + 3H_2 \rightleftarrows CH_4 + H_2O \qquad \Delta H_{298K} = -205.9 kJ/mol \tag{8}$$

Water gas shift reaction:

$$CO + H_2O \rightleftarrows CO_2 + H_2 \qquad \Delta H_{298K} = -41.2 kJ/mol \tag{9}$$

Therefore the only species present at equilibrium are fuel ($C_a H_b O_c$) steam (H_2O) hydrogen (H_2), carbon monoxide (CO), methane (CH_4), carbon dioxide (CO_2), water (H_2O) and graphite (C). Graphite is formed via the Boudouard reactions scheme from carbon monoxide at the catalyst surface. This reformer process is well suited of steady-state operation and can deliver relatively high concentrations of hydrogen. The most important parameter of reforming is the initial gas composition consists in fuel and steam, i.e. $C_a H_b O_c + S/C\, H_2O$ in eq.(10), where the steam-to-carbon ratio, S/C is defined as:

$$S/C = \frac{n_{H_2O}}{a \cdot n_{C_a H_b O_c}} \tag{11}$$

where a indicates the number of carbon atoms in the hydrocarbon. The electrochemical charge-transfer reactions in a SOFC take place in the membrane-electrode assembly (MEA). During this process, the Gibbs free energy (or chemical potential energy) of the global reaction of fuel and oxidizer is converted into electricity. The reversible cell potential (Nernst Potential) E_{rev} between fuel and oxidizer streams is calculated as:

$$E_{rev} = -\frac{\Delta G^{o}}{n_e F} + \frac{RT}{n_e F}\ln\left(\frac{p_{H_2} p_{O_2}^{1/2}}{p_{H_2O}}\right) \quad (12)$$

where $\Delta G°$ is the is the standard-state Gibbs free energy change associated to the global oxidation reaction occurring in the cell anode-side, i.e. $H_2 + ½O_2 \rightarrow H_2O$. E_{rev} is also used to predict the open circuit voltage, OCV. It is important to recall that as air passes through a fuel cell, the oxygen is used, and so the partial pressure will be reduced. Similarly, the fuel partial pressure will often decline, as the proportion of fuel reduces and reaction products increase. Besides, parasitic process may reduce the E_{rev} voltage. In practice lower OCV values are measures compared to those calculated by Eq. (9). The reversible potential, however, varies along the channel length as the fuel is depleted and diluted.

The decrease in power density is due to the fuel dilution effect; diluted fuel results in a lower average current density and for the cases studied here power density solely depends on the current density due to the constant operating voltage during data logging. The Nernst potential is the voltage which drives reversible electrode reactions. This reversible voltage, generated by the overall cell reaction, is a function of the local temperature, pressure, and reactant concentrations. As reactants are utilized, their concentrations change. Since the Nernst potential is dependent upon the concentrations of reactants, it varies with the degree of utilization. Because of depletion and dilution of the fuel and oxidizer streams, this potential can vary along the length of the cell. Each of the over-potentials increases with increasing current density. Irreversible voltage loss is mainly a function of current density and stack temperature. Since these parameters are equivalent in each stack, it is assumed that the Nernst potential of each stack would be reduced by the same amount.

The maximum SOFC efficiency was calculated as:

$$\eta = \frac{qE}{\Delta H^{o}} \quad (12)$$

where F is the Faraday constant, E_{rev} is the reversible cell potential described in eq. (13) and ΔH^{o} is the standard enthalpy change associated to the global oxidation reaction occurring in the cell anode-side, i.e. $H_2 + ½O_2 \rightarrow H_2O$.

3.1 Model validation

The chemical equilibrium model was validated comparing the code developed in EES – Engineering equation

solver – and the CEA-Nasa computer program [22]. The results are shown in table 1. In the calculation only species with molar fraction more than 5.0E-06 is considered. The error between the EES model and the CEA-Nasa computer program reference was computed as a relative difference which takes the "sizes" of the molar fractions into account. The comparison is expressed as a ratio and is a non-dimensional number expressed as percentages.

$$Diff\ \% = \frac{\left|X_{CEA} - X_{EES}\right|}{\left(\left|X_{CEA}\right| + \left|X_{EES}\right|\right)/2} \cdot 100 \tag{14}$$

4. Results

4.1 Minimum reactants S/C ratio comparison

The minimum steam-to-carbon ratio was determined imposing carbon activity, a_c in Eq. (6) equal to unity.

$$a_c = e^{-(\mu_c^0 + \lambda_c)/RT} = 1 \tag{15}$$

This ensures that the molar fraction of C (graphite) is 0 in the considered temperature range.

Figure 1 shows the minimum steam to carbon ratios at temperature between 250 and 1000°C for all chosen fuels. This temperature range was chosen as representative because it includes both the steam reforming and the solid oxide fuel cell operating temperature ranges. With an increasing carbon to hydrogen ratio, the required S/C increases.

The carbon deposition region for methanol lies at lower temperatures while the region for methane lies at intermediate and higher temperatures. The amount of H_2O (g) formed from the methanol-based fuels shown in figure 1 is much higher than that from the methane-based. This feature may be understood as alcohols could be regarded as hydrated hydrocarbons. Therefore, compared to alkanes (C_nH_{2n+2}), less amount of H_2O is needed to prevent carbon deposition especially at higher temperature.

Methanol has a smaller area of carbonization than all other cases because it contributes the minimum number of carbon atoms per mole and requires the smallest stoichiometric factor for complete reforming.

With increasing carbon number of alcohols, the number of hydrogen and oxygen per carbon atom in an alcohol molecule decreases. This reveals that the temperature region of carbon formation slightly expanded with increasing carbon number, so that carbon deposition is thermodynamically expected.

SOFCs generally operated at temperatures above 800°C. However, the stack could also encounter carbon deposition during preheating and pretreatment processes of fuel gases between room temperature and the operational temperature. In the SOFC temperature range of operation, the "driving force" for the carbon deposition reaction decreases with temperature. In practice, carbon deposition may be highly dependent also on kinetics. In fact, higher reforming reactivity occurs at high temperature and inlet steam concentration.

In figure 2, conversion at equilibrium is calculated by solving the coupled set of equations for minimum steam-to-carbon ratio at each specific temperature. Considering product distribution from the steam reforming, the yield of hydrogen production and carbon monoxide fraction increases with increasing temperature, whereas the carbon dioxide and methane production fraction decreases. Even if there is an uncertainty in choosing a single temperature to represent a real reformer which will have temperature differences among multiple catalyst tubes, an equilibrium analysis will still provide a more realistic estimation compared to other methods such as the extent of reaction.

The steam, hydrogen and carbon dioxide fraction increases with increasing inlet steam concentration, whereas the carbon monoxide fraction decreased. The yield of methane production is reduced at higher temperatures. It should be noted that the changes the fractions of hydrogen, carbon monoxide, and carbon dioxide are mainly due to the influence of the mildly exothermic water – gas shift reaction ($CO + H_2O \rightarrow CO_2 + H_2$), whereas the decrease of methane production is due to the further reforming to carbon monoxide and hydrogen. Alcohols show very similar molar fraction composition at high temperatures. The higher the molar carbon content is in the fuel, the higher the reforming factor at a given temperature.

4.2 Steam reforming heat duty

Due to the endothermic nature of the overall reactions, the steam reforming of hydrocarbons requires a significant heat input to obtain the desired conversion to hydrogen. In this study, we define the heat duty as the heat required for the reforming reactions plus the heat required to heat the fuel to the required reforming temperature and the heat input to generate steam:

$$\dot{Q}_{Duty} = \Delta H^{T}_{Reac} + \Delta \dot{Q}^{25\rightarrow T}_{Fuel} + \Delta \dot{Q}^{25\rightarrow T}_{H2O} \tag{16}$$

In figure 3 the heat required to preheat fuel and water to the reforming temperature is shown (i.e. $\dot{Q}^{25^0C\rightarrow T}_{Fuel} + \dot{Q}^{25^0C\rightarrow T}_{H_2O}$). As the amount of steam is always larger in the fuel stream, this heat input is mainly used to generate steam. At high temperatures, a lower S/C-ratio is required. A lower amount of steam leads to less heat

required and hence an almost flat trend of the heat duty over a large range of temperatures.

In figure 4, the enthalpy of reaction at different temperatures ΔH^{T}_{Reac} is shown. Higher temperatures require more heat for the reforming process. At low temperature ranges, the mildly exothermic methanation (Eq. 11) and shift reactions (Eq. 12) are more dominating than the steam reforming reaction causing negative values for ΔH^{T}_{Reac}. At high temperatures, n-octane shows higher heat of reaction due to greater bond energy of this molecule.

4.3 Cell performance and efficiency

The electro motive force is governed by equation (12) which depends on the types of fuel. The decrease in H_2 concentration is one of the main reasons explaining lower EMF and lower electrochemical performance [14]. The influence of temperature on the hydrogen partial pressure is logarithmic, which means that the voltage is not largely affected by the fuel composition but only depends on the working temperature as shown in figure 5.

4.4 Experimental test

Steam reforming product compositions were used to evaluate and compare SOFC performance with different hydrocarbons. The anode gas composition was calculated at chemical equilibrium at 850°C. The used compositions are reported in Table 2. The table also lists the steam to carbon ratio (S/C) at equilibrium for the reforming reaction. The minimum S/C-ratio to thermodynamically avoid carbon formation was chosen in each case scenario. Since at high temperatures methanol and ethanol give same equilibrium composition, from now only the ethanol composition is considered. For this reason only ethanol was considered for the experimental analysis.

The test was performed in a single SOFC cell, electrolyte supported. Fuel gas was normalized in order to have the same low heating value for each composition. Reference flow rate of hydrogen was selected equal to 36,14 mol/min. Air rate at cathode was kept constant during all tests at 120,48 mol/min. Both these values are indicated by cell supplier, Next Cell, as operative condition of the cell. With these fuel and air flow streams, utilization of fuel (U_f) is 20% at 500 mA/cm^2 and the utilization of oxygen (U_{ox}) at same current density is 14%. While U_{ox} is similar with operative conditions U_f is much lower than common values (around 0,8). Furnace temperature was fixed to 850 °C which is the temperature of operation of an electrolyte supported SOFC. Obtained gas stream values are reported in Table 3. Reference H_2 standard composition was used to compare results.

The cell is located inside a furnace and both cell and furnace temperatures are monitored. During the tests,

temperature, gas flow rates, current and voltage are measured and controlled. Inlet anode gas is heated up using an electric heating cable which regulates the fuel inlet temperature in order to avoid steam condensation.

The anode current collector mesh is realized in nickel while at the cathode side it is made of silver. A sealing is placed around the mesh to avoid gas leakages. An electronic load in series with a power supply permits cell current control and measurement. The test rig includes a cell voltage sensor and thermocouples located inside the cell housing and along the gas line. The cell temperature was calculated as the average between the temperatures measured inside the anodic and cathodic housing. Finally, the mechanical load is placed over the cathode and is regulated to obtain the required compression of the fuel cell assembly. Most important cell specifications are reported in Table 4.

Cell startup was carried out by following the procedure provided by the supplier. Selected gas compositions were delivered to the cell for one hour at open circuit voltage (OCV) to achieve voltage and temperature stabilization; after this phase, a complete cell polarization curve was performed. Each polarization was executed starting from OCV and increasing current with a 0.5A step corresponding to 38.8 mA/cm^2. Each polarization point was kept for 2 minutes in order to reach steady-state operation. The procedure was interrupted when 0.6 V was reached. Data were logged at 0.5 Hz and grouped for each step of current. Average values for each condition was calculated and the distribution of data was verified to have a standard deviation below 1%. Polarization was performed in forward and reverse mode to reduce cell stress and to verify any hysteresis. No significant variation was ever measured between the two curves.

Cell voltages and temperatures are reported in Figure 6. Reformed fuels produce similar OCV values due to the fact that the sum of concentration of inert gases, such as H_2O and CO_2 that do not participate in the electrochemical reactions. This is in accordance thermodynamic calculation results presented OCV ranges around 1.1 V. A detailed data fitting with the thermodynamic model was not considered relevant for the scope of this research as the purpose of this study was to explore fuel cell response to different fuels rather than a full polarization curve model validation.

As expected, the anode temperature is higher when using pure hydrogen as fuel compared to other fuels. In this case, the heat generated by the electrochemical reaction is not absorbed by the endothermic steam reforming reactions like in the other cases.

To have a detailed analysis of the results, polarization data were plotted as the difference between each of the three tested compositions which were compared with the reference. A voltage-decay was thus defined as the difference between the measured data and the reference composition for each value of current density. In figure

7 these results are plotted. It is important to note that all positive and negative decays are below 5 mV, so the results are quire similar. Going into details we can observe that the OCV values are affected by the hydrogen concentration and ethanol and gasoline, where the hydrogen concentration is smaller and differs from methane. Specifically, gasoline and ethanol decay at OCV compared to reference is higher due to smaller H_2 concentration. This difference is reduced along polarization curve. We can imagine that when water is produced due to the electrochemical reaction, the shift reaction contributes to reduce difference in pure hydrogen concentration. For values above 100 mA/cm^2 the decay becomes negative, meaning that reformed fuels perform better than the reference. This difference is mainly due to the fact that the reference test was performed after the others and the cell and a small degradation occurred.

In conclusion, the experimental activity shows that the defined compositions subject to these conditions have similar effect both in terms of performance and in terms of thermal balance. A reduction of current affects polarization performance mainly with an increase of OCV and an increase of internal resistance with a general effect of reducing performances. If the reforming temperature is reduced, the composition will have minimum change in terms of the inlet gas LHV and consequently in terms of performance. The parameter that strongly affects the performance in the cell is the steam content: If reforming conditions are kept so to have minimum steam content, the hydrogen concentration and the OCV value will have optimal conditions in terms of energy performance.

Conclusion

A major concern when operating SOFCs with hydrocarbons or syngas fuels is the formation of solid carbon through undesired side reactions. The mechanisms for solid carbon deposition are not yet fully known, but they will almost certainly depend on the operating conditions in the cell, e.g., temperatures and most notably the steam content in the fuel stream.

Using a chemical equilibrium model based on Gibbs free energy minimization of the gas mixture, the amounts of reforming reaction products have been calculated for various SOFC fuels. The product compositions have been used to compare the SOFC performance during an experimental test on a single cell. In order to consistently compare the system performance using different fuels for each case study. Minimum steam-to-carbon ratios in terms of chemical equilibrium to prevent carbon formation where used.. The developed model can be reproduced in any numerical equation solver making it adaptable to different software platforms.

The experimental tests confirms the simulation revealing that the steam reformed product composition show similar electromotive force (EMF) output for optimal conditions. In fact, at temperatures exceeding 800°C, the

gas composition is dominated by hydrogen and carbon monoxide for any fuel considered. Besides the cell polarization curves showed similar performance for different fuels if a high degree of fuel pre-reforming is considered.

This leads to conclude that most of the burden in system performance is accounted for by the heat requested for the fuel reforming process. Specifically, heat for steam generation is major contributor to the heat loss in the energy system. The highest amount of heat required for the steam production was observed in the case gasoline surrogate was used as a fuel. Besides if reforming conditions are kept close to minimum steam content, system energy performance will be improved.

Acknowledgment

The experimental test was conducted at the Fuel Cell lab – University of Perugia, Italy, thanks to the European project H2FC (FP7- Infra-2011-1.1.16 GA n. 284522).

References

[1] EG&G Technical Services I. Fuel Cell Handbook. U.S. Dept of Energy; 2004.

[2] Liso V, Nielsen MP, Kær SK. Ejector design and performance evaluation for recirculation of anode gas in a micro combined heat and power systems based on solid oxide fuel cell. Appl Therm Eng 2013;54:26–34.

[3] Xu H, Dang Z, Bai B-F. Analysis of a 1 kW residential combined heating and power system based on solid oxide fuel cell. Appl Therm Eng 2013;50:1101–10.

[4] Ahluwalia RK, Wang X. Buildup of nitrogen in direct hydrogen polymer-electrolyte fuel cell stacks. J Power Sources 2007;171:63–71.

[5] Elmer T, Worall M, Wu S, Riffat SB. Emission and economic performance assessment of a solid oxide fuel cell micro-combined heat and power system in a domestic building. Appl Therm Eng 2015.

[6] Pilavachi PA, Stephanidis SD, Pappas VA, Afgan NH. Multi-criteria evaluation of hydrogen and natural gas fuelled power plant technologies. Appl Therm Eng 2009;29:2228–34.

[7] Shekhawat D, Spivey JJ, Berry DA. Fuel Cells: Technologies for Fuel Processing: Technologies for Fuel Processing. Elsevier Science; 2011.

[8] Wen H, Ordonez JC, Vargas JVC. Optimization of single SOFC structural design for maximum power. Appl Therm Eng 2013;50:12–25.

[9] Coutelieris F. The importance of the fuel choice on the efficiency of a solid oxide fuel cell system. J Power Sources 2003;123:200–5.

[10] Douvartzides SL, Coutelieris F a., Demin a. K, Tsiakaras PE. Fuel options for solid oxide fuel cells: A thermodynamic analysis. AIChE J 2003;49:248–57.

[11] Sasaki K, Hori Y, Kikuchi R, Eguchi K, Ueno a., Takeuchi H, et al. Current-Voltage Characteristics and Impedance Analysis of Solid Oxide Fuel Cells for Mixed H[sub 2] and CO Gases. J Electrochem Soc 2002;149:A227.

[12] Sasaki K, Teraoka Y. Equilibria in Fuel Cell Gases: : I. Equilibrium Compositions and Reforming Conditions. J Electrochem Soc 2003;150:A878.

[13] Sasaki K, Teraoka Y. Equilibria in Fuel Cell Gases II. The C-H-O Ternary diagram. J Electrochem Soc 2003;150:A885.

[14] Sasaki K, Watanabe K, Teraoka Y. Direct-Alcohol SOFCs: Current-Voltage Characteristics and Fuel Gas Compositions. J Electrochem Soc 2004;151:A965.

[15] Liso V, Nielsen MP, Kær SK. Evaluation of Different System Configurations for Solid Oxide Fuel Cell-Based Micro-CHP Generators in Residential Applications. Eur. Fuel Cell Forum, 2009, p. 1–14.

[16] Yang Y, Du X, Yang L, Huang Y, Xian H. Investigation of methane steam reforming in planar porous support of solid oxide fuel cell. Appl Therm Eng 2009;29:1106–13.

[17] Rostrup-Nielsen J, Christiansen LJ. Concepts in syngas manifacture. 2011.

[18] White WB, Johnson SM, Dantzig GB. Chemical Equilibrium in Complex Mixtures. J Chem Phys 1958;28:751.

[19] Lima da Silva A, Malfatti CDF, Müller IL. Thermodynamic analysis of ethanol steam reforming using Gibbs energy minimization method: A detailed study of the conditions of carbon deposition. Int J Hydrogen Energy 2009;34:4321–30.

[20] Cimenti M, Hill JM. Direct Utilization of Liquid Fuels in SOFC for Portable Applications: Challenges for the Selection of Alternative Anodes. Energies 2009;2:377–410.

[21] Klein S, Nellis G. Thermodynamics. Cambridge University Press; 2011.

[22] Nasa. CEA (Chemical Equilibrium with Applications) 2010.

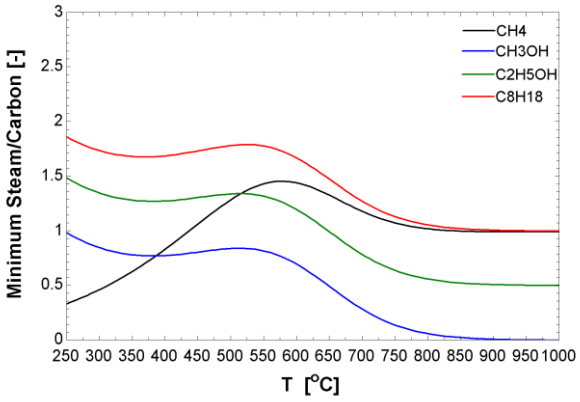

Figure 1 Minimum Steam to carbon ratio of the reforming reactants at different temperatures

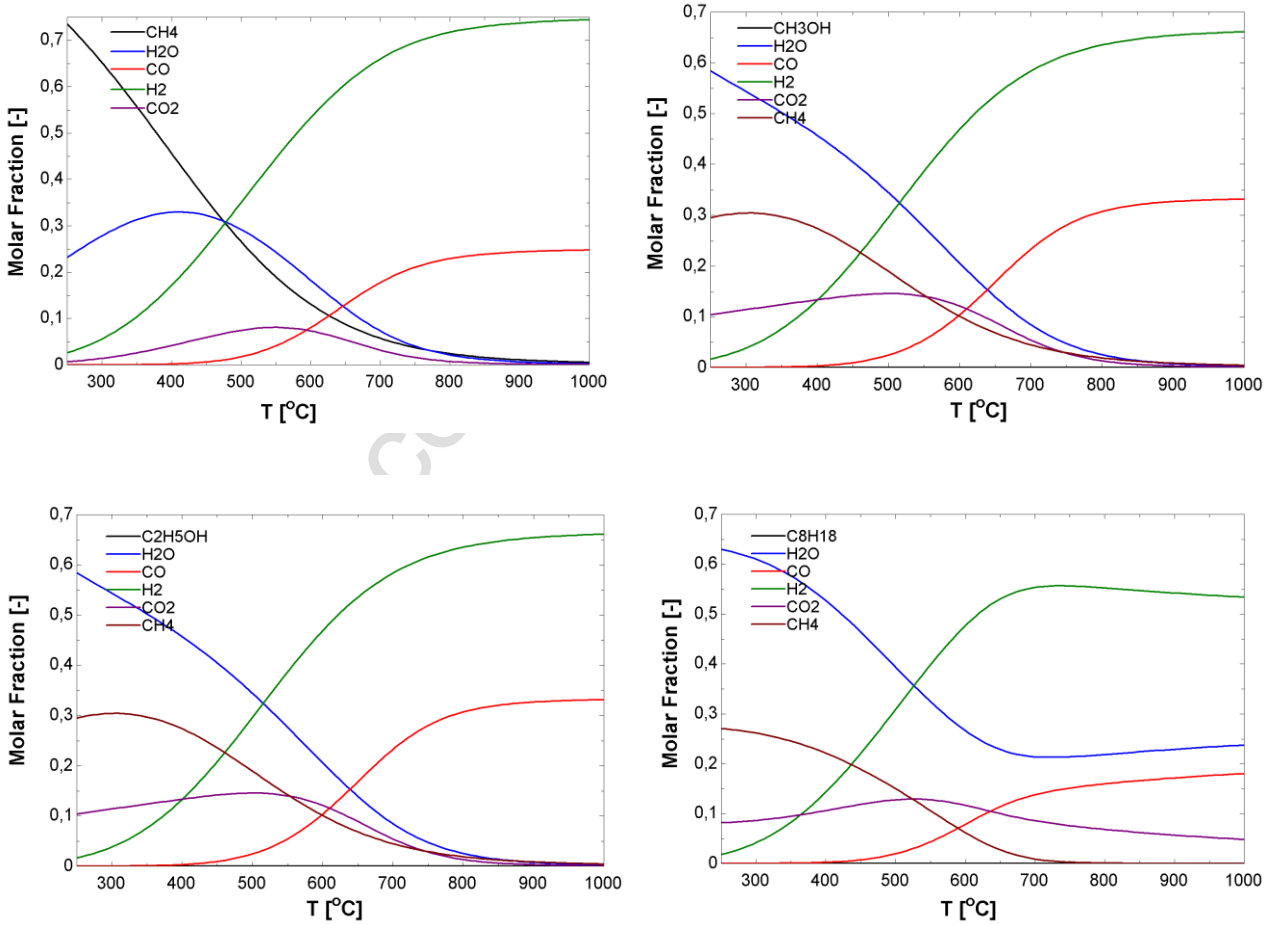

Figure 2 Gas compositions at equilibrium for CH_4, CH_3OH, C_2H_5OH and C_8H_{18} when minimum steam to carbon ratio of the reactant is considered.

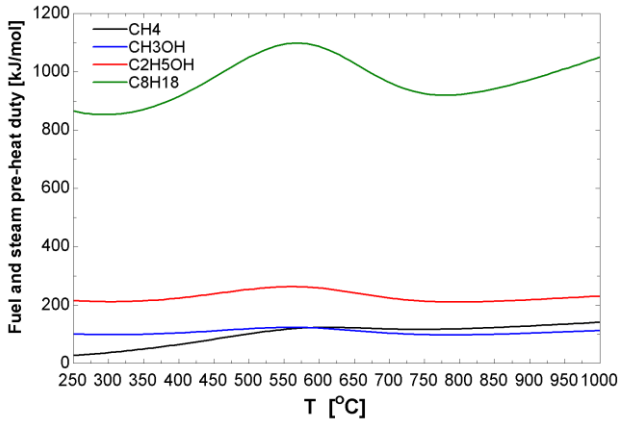

Figure 3 Heat required to pre-heat fuel and water up to the reforming temperature in case of minimum steam to carbon ratio of the reactant.

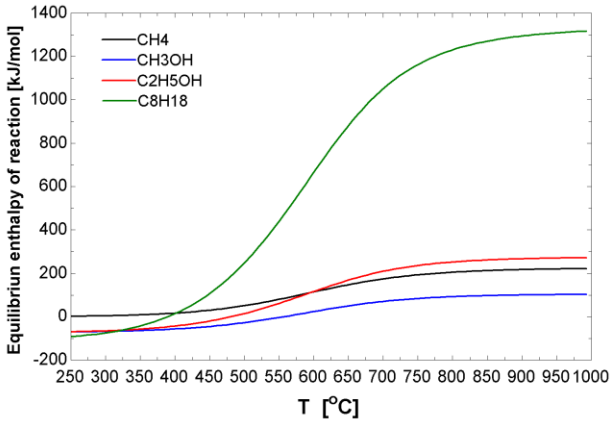

Figure 4 Steam reforming heat of reaction of different fuels at different temperatures.

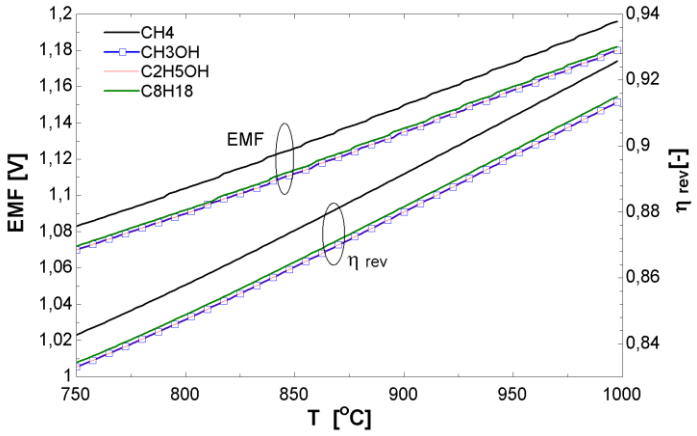

Figure 5 Cell electromotive force e.m.f and reversible efficiency when fuel composition produced by reforming process with minimum steam to carbon ratio.

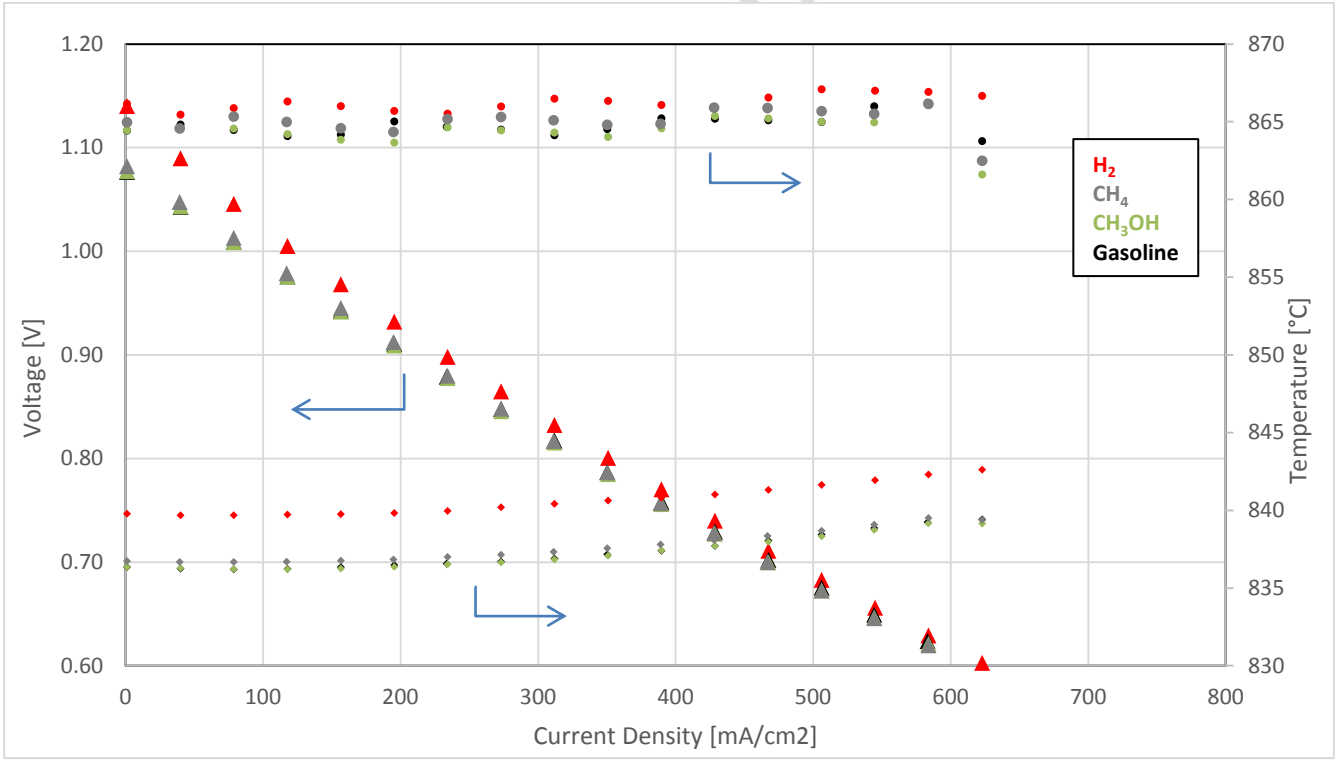

Figure 6 Polarization curves and anode and cathode temperatures of tested gas compositions

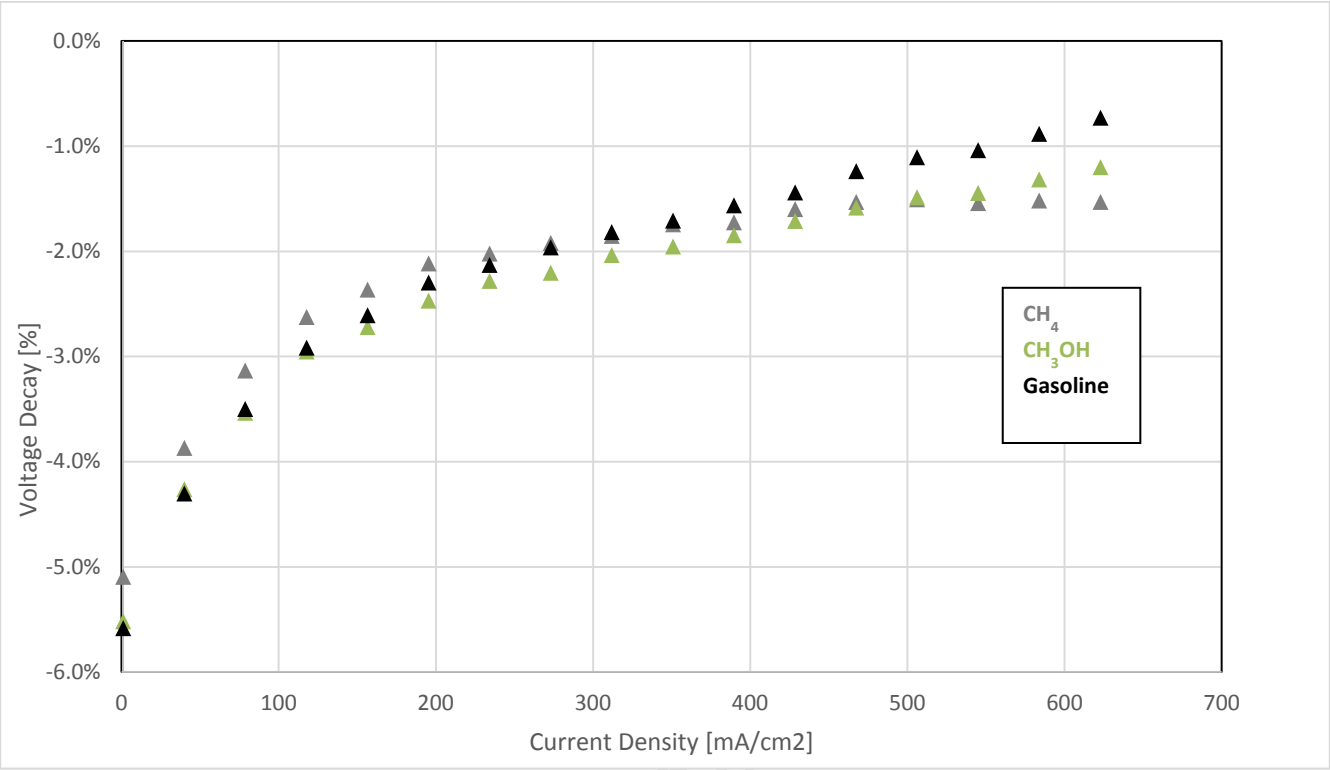

Figure 7 Voltage decay of each composition tested compared to pure hydrogen.

Table 1: Comparison of the results obtained by the model and CEA-NASA code for CH4 MeOH, EtOH and C8H18 at (Steam/Fuel of Reactant=2.5; P=1atm)

Molar Fraction (*X*)	500°C			800°C		
	CEA-NASA	Model	Diff%	CEA-NASA	Model	Diff%
CH4	0.142	0.142	0.154	0.001	0.001	1.098
H2O	0.414	0.413	0.103	0.222	0.222	0.020
CO	0.013	0.013	0.383	0.129	0.129	0.008
CO2	0.078	0.078	0.102	0.052	0.052	0.038
H2	0.352	0.352	0.130	0.596	0.596	0.008
C	0	0		0	0	
CH3OH	0	0		0	0	
CH4	0.079	0.079	0.238	0.000	0.000	0
H2O	0.489	0.489	0.081	0.369	0.369	0.012
CO	0.014	0.014	0.568	0.096	0.096	0.021
CO2	0.117	0.117	0.008	0.085	0.085	0.023
H2	0.299	0.300	0.130	0.449	0.449	0.015
C	0	0		0	0	
C2H5OH	0	0		0		
CH4	0.171	0.200	15.512	0.001	0.001	8.612
H2O	0.365	0.333	9.406	0.186	0.146	24.029
CO	0.023	0.025	11.794	0.184	0.209	13.005
CO2	0.141	0.148	4.1818	0.066	0.056	15.127
H2	0.299	0.294	1.646	0.563	0.586	3.975
C	0	0		0	0	
C8H18	0	0		0	0	
CH4	0.226	0.200	12.305	0.0197	0.020	1.098
H2O	0.139	0.130	7.6322	0.0088	0.012	0.018
CO	0.007	0.007	3.3426	0.1193	0.116	0.008
CO2	0.020	0.020	1.3138	0.0020	0.003	0.038
H2	0.264	0.300	12.683	0.5685	0.561	0.008
C	0.343	0.346	1.0421	0.2862	0.288	0.008

Table 2 Anode inlet gas composition for experimental activity at 800°C considering minimum S/C of the reactant

	H_2	CO	CO_2	CH_4	H_2O	Inlet S/C ratio
CH_4 (Methane)	71.9%	23.01%	0.71%	2.36%	2.06%	1.01
CH_3OH (Methanol)	63.6%	30.83%	1.27%	1.85%	2.44%	0.05
C_2H_5OH (Ethanol)	63.6%	30.83%	1.27%	1.85%	2.44%	0.55
C_8H_{18} (Gasoline Surrogate)	64.9%	29.61%	1.17%	1.92%	2.40%	1.05

Table 3 Anode inlet gas composition for experimental activity at 850°C

	Flows mol/min					Total Anodic [mol/min]	Air [mol/min]
	H_2	CO	CO_2	CH_4	H_2O		
CH_4	24.90	7.97	0.24	0.82	0.75	34.68	120.48
C_2H_5OH (Ethanol)	22.58	10.94	0.45	0.66	0.76	35.39	120.48
C_8H_{18} (Gasoline Surrogate)	22.95	10.47	0.41	0.68	0.76	35.28	120.48
Hydrogen	36.14	0	0	0	0.79	36.14	120.48

Table 4 cell specifications

Cell type	Electrolyte Supported – Planar
Dimension	5 cm x 5 cm
Active area (measured)	3.9 cm x 3,3 cm = 12.87 cm^2
Anode	50 µm Ni-GDC/Ni-YSZ multi-layer
Electrolyte	150 µm Ni-GDC/Ni-YSZ
Cathode	50 µm LSM/LSM-GDC multi-layer